Relating colloidal particle interactions to gel structure using Brownian dynamics simulations and the Fuchs stability ratio

M. Mellema, J. H. J. van Opheusden, and T. van Vliet

Citation: J. Chem. Phys. **111**, 6129 (1999); doi: 10.1063/1.479956
View online: http://dx.doi.org/10.1063/1.479956
View Table of Contents: http://jcp.aip.org/resource/1/JCPSA6/v111/i13
Published by the American Institute of Physics.

Relating colloidal particle interactions to gel structure using Brownian dynamics simulations and the Fuchs stability ratio

M. Mellema[a)]
Food Physics, Department of Food Technology and Nutritional Sciences, Wageningen University, Bomenweg 2, 6703 HD Wageningen, The Netherlands

J. H. J. van Opheusden
Mathematical Methods and Models, Department of Agricultural, Environmental, and System Technology, Wageningen University, Dreijenlaan 4, 6703 HA Wageningen, The Netherlands

T. van Vliet
Food Physics, Department of Food Technology and Nutritional Sciences, Wageningen University, Bomenweg 2, 6703 HD Wageningen, The Netherlands

(Received 12 April 1999; accepted 29 June 1999)

Brownian dynamics simulations of aggregation of hard-sphere dispersions at intermediate volume fractions (~3–10 vol%) have been performed. A long-range activation energy for aggregation was incorporated. The bonds formed were irreversible and flexible. Cluster growth rate and fractal properties of the gel matrix could be related to particle interactions by using a Fuchs stability ratio W_F. Although this approach is expected to apply only to the very early stages of gelation, W_F was shown to be a useful parameter, especially for predicting gel matrix parameters like the fractal dimensionality D_f (which is a measure of the compactness of the clusters in the intermediate or fractal length scale regime) and the correlation length ξ (which is a measure of the average gel pore size). The number of aggregates, N_{agg}, was found to be a convenient measure of the stage of aggregation for the range of volume fractions and interactions studied. For high values of W_F, the value of D_f was more generic (i.e., less dependent of W_F or φ). In addition, the fractal parameters were less dependent on W_F at higher φ. These observations can be explained by the limited formation of (diffusion-kinetics type) depletion zones in the presence of repulsive barriers compared to purely attractive systems. © *1999 American Institute of Physics.* [S0021-9606(99)51036-2]

INTRODUCTION

In recent years, several Brownian Dynamics (BD) simulation studies have been published on the formation and properties of particle gels.[1–8] The various studies differ with respect to the interaction potential used, the freedom for rearrangement, volume fraction, etc. Here we present a study on aggregation and gelation of spherical particles at intermediate volume fractions (around 3–10 vol%), using a BD simulation model with short-range irreversible bonding and intermediate-range repulsive pair-interactions. We will focus on the effect of delayed aggregation due to an incorporated repulsive barrier on the aggregation rate on the evolution of the fractal structure[3,9] of the aggregates and gel matrix, at different volume fractions. Even though in practical systems, e.g., casein gels, often a repulsive barrier at intermediate distances is present during aggregation, this aspect has not been thoroughly studied before.

The simulation results are compared to rennet-induced gelation of skim milk. In milk, casein particles are present which are protected against aggregation by a hairy layer comprising of the C-terminal ends of κ-casein molecules. The hairs can be ''removed'' by rennet enzymes,[10] and attractive forces become operative.

A gel is only obtained if the aggregation is irreversible or above a certain percolation threshold volume fraction.[11] For casein micelle gelation no threshold value can be found,[12] hence the aggregation is probably largely irreversible. Aggregation rates found in casein dispersions and milk are low, probably because a ''hairy layer'' remains even after renneting.[13–15] Subsequently the gel fractal dimensionalities are relatively high[9,16] (even higher than expected for reaction-limited aggregation[17]). It may thus be illustrative to incorporate (high) repulsive barriers in the simulations.

We will show that the Fuchs stability ratio[18] can be a useful parameter in predicting the fractal characteristics of the simulated gels. The relevant characteristics of the particle interactions can be approximated by this ''stickiness'' parameter if only limited rearrangements are allowed. Furthermore, by pointing out some differences between results from the simulations and from experiments on milk gels, we will show the importance of gel matrix rearrangements.

BROWNIAN DYNAMICS MODEL

The BD model is based on a Langevin-type equation of motion for each of the macroscopic particles with a fluctuating random force added to account for the thermal collisions of the solvent molecules with the particle. The solvent is considered as a continuum. We keep track of N hard-core spheres in a cubic box with edges set equal to R, using pe-

a)Author to whom correspondence should be addressed. Electronic mail: Michel.Mellema@Phys.FdSci.WAU.NL. Fax: +31 317 483669.

riodic boundary conditions. All parameters corresponding to sizes or distances are normalized to the radius of one spherical particle and all parameters corresponding to energies are normalized to units of kT.

The resulting force on a particle i, F_{res}, is given by the Langevin equation:[19]

$$F_{\mathrm{res}}=m\frac{d^2}{dt^2}r_i=\sum_j F_{ij}(r_{ij})+R_i+H_i, \tag{1}$$

where t is the time, F_{ij} is the net force of interaction between the pair of particles i and j, R_i is the random (Brownian) force, H_i is the Stokes friction force acting on particle i and r_i is the position of particle i, and r_{ij} is the relative position of particle i to particle j.

The particle pair-interactions (represented by F_{ij}) are described using a potential $u(r)$. The force F_{ij} is taken to be constant over a center-to-center distance $2.1<r<D$:

$$u(r)=\begin{cases}0 & r\geqslant D\\ F_{ij}(r-D) & D_{\mathrm{bond}}<r<D,\\ 0 & 2<r<D_{\mathrm{bond}}\end{cases} \tag{2}$$

where D_{bond} is the bonding distance (always set to 2.1) and D is the maximum interaction distance (ranging from 2.1 to 3.3). In this study, the parameter F_{ij} ranges from 0 to -25, implying the interactions are repulsive. Note that the hard-core repulsion implies formal $u(r)=\infty$, for $r<2$.

Once a bond is formed it is irreversible. The points at which the bonds are attached to the particle surfaces are fixed and the angles between all bond attach points on the same particle are fixed too. The relative particle motion is restricted such that the surface-to-surface bond length does not exceed the maximum specified bond length $D_{\mathrm{string}}=0.1$, but it can be less also, which gives a certain bond ''flexibility''.[8]

The liquid drag force, H_i, is proportional to the particle velocity:

$$H_i=\frac{dr_i}{dt}\gamma, \tag{3}$$

where $\gamma(=6\pi\eta_0)$ is the Stokes drag and η_0 is the solvent shear viscosity. Note that the particle radius $a=1$. Many-body hydrodynamic interactions are neglected.

Equation (1) is solved numerically to extract the movement of the particles, using a constant timestep Δt. We chose this Brownian timestep much larger than the relaxation time of the particle velocity, but small enough to ensure that the interaction forces do not change significantly during one timestep. Using the Euler forward method[19] to solve the remaining first-order differential equation, we arrive at:

$$\Delta r_i(t+\Delta t)=\frac{\Delta t}{\gamma}\left(\sum_j F_{ij}(t)+R_i(t)\right). \tag{4}$$

The effect of the random force R_i is a translational displacement which, on the average, obeys Einstein's law for an isolated particle. For instance in the x-direction this gives us:

$$\Delta x_i^R(t+\Delta t)=N_s\sqrt{6D_c\Delta t}, \tag{5}$$

where $D_c(=1/\gamma)$ is the diffusion coefficient, which is normalized to 1. The parameter N_s is a uniform random number on $(-1,1)$, so its variance is 1/3. The dimensionless root-mean-square displacement in the absence of interactions is $\langle|\Delta x_i^R|\rangle=\sqrt{(2D_c\Delta t)}$. For all simulations we fixed $\sqrt{(2D_c\Delta t)}$ at 0.004, which is small enough also for the steeper potentials. If the number of particles is N, in one timestep $3N$ numbers corresponding to all three directions (x,y,z), are drawn. This means that we have uncorrelated distributions (i.e., no hydrodynamic interactions between the particles) for $F_{ij}=0$. The number of steps which the simulation has passed, is given by $N_{\Delta t}$. The parameter $N_{\Delta t}$ is a direct measure of time.

Apart from the translational diffusion the individual particles also undergo rotational diffusion. The rotational motion is governed by a diffusion coefficient D_R. (particle radius $a=1$, $kT=1$):

$$D_R=\frac{3D_c}{4}. \tag{6}$$

The implementation of the rotational diffusion is quite similar to that of translational diffusion, with small uniformly random rotations of each particle as to satisfy Eq. (6). Rotational diffusion of the clusters is generated by the different translations of the individual particles combined with the constraints. These constraints, both the hard-core repulsion and the finite length strings, which may be violated by the particle displacements, are satisfied by a SHAKE-like procedure,[19] iteratively running over all violated constraints, and removing these by moving and rotating the involved particles.

AGGREGATION KINETICS

Meakin[20] defined two types of aggregation which differ with respect to the ''probability of bonding'' due to different particle interactions. In Diffusion-Limited Cluster Aggregation[21] (DLCA) each particle (or cluster) encounter leads to bonding. For Reaction-Limited Cluster Aggregation[17] (RLCA), there is a low chance of bonding (upon particle encounter) so on average a large number of particle encounters are needed for bonding.

A higher degree of reaction limitation causes a delay in the aggregation process and the structures formed are usually more compact, i.e., have higher fractal dimensionality.[22] In order to quantify the relation between particle interactions and fractal gel structure, we introduce the Smoluchowski[23] and Fuchs[18] concept of the stability ratio W, which measures the effectiveness of a potential barrier in preventing colloidal particles from aggregating. The basic definition of W is given by Smoluchowski (for repulsive hard spheres):

$$W=\frac{\text{average time for bonding with repulsion}}{\text{average time for bonding without repulsion}}. \tag{7}$$

The reciprocal of W $(=1/W)$ is the sticking probability of the encountering particles. For our simulations, this theory can only be expected to apply to the first few aggregation steps or, equivalently, to a few times the time required for the number of separate particles to be reduced to half of the

initial value. After this ''Smoluchowski-regime'' the shape and dimensions of the aggregates formed will influence the rate of the ongoing aggregation.

According to Smoluchowski,[23,24] the particle flux for dimerisation of a single pair of identical hard spheres equals:

$$J_0 = 2aD_c\varphi, \tag{8}$$

where φ is the particle bulk volume fraction. According to Fuchs,[18,24] the particle flux for a single pair of identical spheres *with* a potential force between the particles equals:

$$J = \frac{D_c\varphi}{\int_{2a}^{\infty} \frac{1}{r^2} e^{u(r)/kT}\, dr}, \tag{9}$$

where r is the particle distance. The probability of bonding, which Fuchs originally called κ, equals J/J_0. We now introduce a Fuchs stability ratio $W_F = 1/\kappa$:

$$W_F = 2a \int_{2a}^{\infty} \frac{1}{r^2} e^{u(r)/kT}\, dr. \tag{10}$$

The integral can be approximated numerically for any shape of the repulsive barrier $u(r)$, defined by the value of the parameters F_{ij} and D.[8] In our case [Eq. (2)] the interaction force (F_{ij}) and range (D) are the important parameters, the bond length (D_{bond}) has only minor influence. This ''theoretical'' W_F will be related to ''experimental'' fractal parameters obtained from the simulations.

POWER-LAW BEHAVIOR

For an ideal fractal aggregate, the following scaling relation can be written:[16,25]

$$\varphi_c = \left(\frac{R}{a}\right)^{D_f - 3}, \tag{11}$$

where φ_c is the density or volume fraction inside the aggregate of size R and D_f is the fractal dimensionality. A 3-D homogeneous object would give $D_f = 3$, which means that φ_c is independent of cluster size. For $D_f < 3$ the density drops with increasing cluster size. At the ''gel point,'' t_{gel}, we assume $\varphi_c = \varphi$ and define $R = R_{\text{gel}}$. Rewriting Eq. (11) leads to:

$$R_{\text{gel}} = a_{\text{eff}} \varphi^{1/D_f - 3}, \tag{12}$$

where a_{eff} is a prefactor equal to an effective particle radius.[12]

In experiments t_{gel} is roughly defined at the point at which the storage modulus G' is systematically larger than the loss modulus G''. The change of the actual R_{gel} with the bulk volume fraction φ is a central subject in the fractal analysis of rheological and permeability data.[16,26]

The mass distribution of an object or an image of the object can be probed by evaluating a pair correlation function $g_2(r)$. In computer simulations all particle positions are known, so $g_2(r)$ is exactly defined. For estimating an effective D_f from the simulations, it is convenient to smooth out short-range oscillations in $g_2(r)$ by integration, leading to:[3,9]

$$n \propto \tilde{n} \left(\frac{r}{2a}\right)^{D_f}; \quad 2a \leqslant r \leqslant \xi, \tag{13}$$

where n is the average number of particles within range r of another particle and ξ is the correlation length. The correlation length ξ is an important parameter because at t_{gel}, it should equal R_{gel}. The prefactor $\tilde{n}$ is defined as the effective average number of particles at $r = 2a$. The procedure of the linear fitting according to Eq. (13) (shown later in Fig. 3) is a plot of $\log(n)$ vs $\log(r)$ and shows how D_f, $\tilde{n}$, and ξ are derived.

The gel matrix is only fractal over a limited range of length scales. The parameter ξ is the upper cutoff length of the fractal regime (or the lower cutoff length of the homogeneous regime at large length scales; $D_f = 3$). In a dispersion of separate particle clusters ξ corresponds to the average cluster separation. In a gel matrix ξ corresponds to the average radius of the gel pores. The values of $\tilde{n}$ gives information on the compactness of the gel matrix at small length scales.

Scaling laws can also be applied to quantify the kinetics of the cluster growth. The kinetics of aggregation can be described by a simple power on the average radius of gyration R_g:[4]

$$R_g \propto t^{\alpha}, \tag{14}$$

where α is a constant depending on sticking probability and volume fraction. In theories on droplet coalescence, the value of α is predicted to be 1/3 (Lifshitz–Slyozov) or 0.2 (Binder–Stauffer). Generally the exponent is in the range ~0.2–0.4. For diffusion-limited growth α equals $1/D_f$ and for reaction-limited growth $R_g \propto e^{\beta t}$, where β is a constant.[27]

Assuming that ξ is proportional to R_g, we should be able to relate the parameter α to the Fuchs stability ratio W_F. In addition, if we define $\xi(t_{\text{gel}}) = R_{\text{gel}}$, we can derive how R_{gel} relates to W_F or the volume fraction and compare this to experimental results. Especially the relation between R_{gel} and φ is important in the fractal analysis [see Eq. (12)] of permeability or rheology data.

RESULTS AND DISCUSSION

Simulations have been performed for various values of D and F_{ij}. For each combination of D and F_{ij}, a value of W_F was calculated. Note that several combinations of D and F_{ij} can lead to the same value of W_F.

A value for W can be derived from the evolution of the total number of bonds in the system, N_{bonds}, with the number of timesteps $N_{\Delta t}$ ($N_{\Delta t}$ is proportional to the time), according to the method described earlier.[8] In this paper, we have also shown that W_F and W are equivalent. This supports the validity of the approach, at least in the early stages of aggregation.

At the start of a simulation, the total number of aggregates $N_{\text{agg}} = 1000$ and $N_{\text{bonds}} = 0$. During a simulation, N_{bonds} increases, N_{agg} decreases, and subsequently the number of free (nonbonded) particles decreases (Fig. 1) and the average number of particles per aggregate increases (Fig. 2). From Fig. 1 we see that at $N_{\text{agg}} = 10$ the number of free particles is approximately zero. So any bonds formed after $N_{\text{agg}} = 10$,

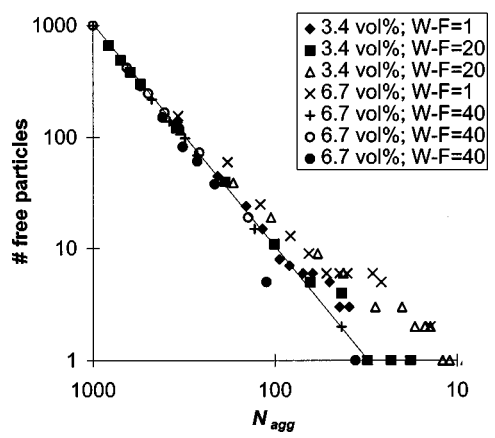

FIG. 1. Number of free (nonbonded) particles as a function of the number of aggregates, N_{agg}, for several combinations of F_{ij} and D.

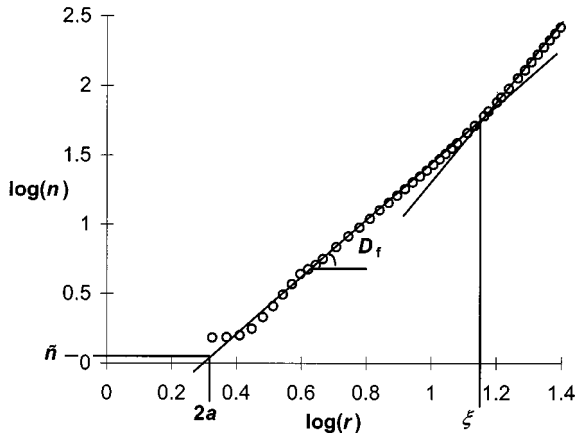

FIG. 3. Example of a determined number correlation function $n(r)$, indicating how the fractal parameters are derived. Volume fraction $\varphi=3.4$ vol%.

can be assumed to be inter- or intracluster. The figure also illustrates the generic behavior of the aggregation process, since the results of simulations of a variety of combinations of φ, F_{ij}, and D ($\varphi=0.034$ or 0.065, $W_F=1$, 20, or 40) nearly coincide on a straight ''mastercurve'' on a double log-scale.

We clearly see from Fig. 2 that already at a stage at which $N_{\mathrm{agg}}=340$, most of the particles are in small aggregates of a size 3 to 5. This presence of a limited amount of single particles during the aggregation process is certainly not unusual for cluster–cluster aggregation. Figure 2 is an average of the results of four simulations, namely $\varphi=0.034$ ($W_F=1$ and 20) and $\varphi=0.065$ ($W_F=1$ and 40); surprisingly, there was no systematic difference between these simulation results. Any difference in R_{gel} at different φ or W_F is probably due to the formation of more tenuous or dense aggregates, and not to a different distribution of the particles over the aggregates (see below). Both Fig. 1 and 2 suggest that the parameter N_{agg} is a good measure of the stage of aggregation for the full range of values of φ and W_F studied.

In Fig. 3 we give an example of the number density correlation function $n(r)$, to indicate how the fractal parameters were derived. Usually the simulated gel structures have a fractal regime over roughly half a decade. The size of the fractal regime decreases as φ increases, because the clusters are smaller at the moment a gel is formed.

An example of the development of the parameters D_f, $\tilde{n}$, and ξ during a simulation (one simulation data set; $W_F=1$, $\varphi=0.034$) is given in Fig. 4. We see that D_f gradually decreases with the decrease in N_{agg}, while $\tilde{n}$ increases. The parameter $\tilde{n}$ can be smaller that 2, because it is derived by extrapolation from the fractal regime.

The evolution of ξ with $N_{\Delta t}$ is shown in Fig. 5 on a log–log scale. It is clear that ξ increases with time. A value for α can be derived from each line (see below, Fig. 6), assuming that $\xi=R$. We found that a semilogarithmic plot [$\log(R_{\mathrm{gel}})$ as a function of t, not shown] of Fig. 5 did not give a linear behavior. So the aggregate radius does not grow exponentially, as expected for pure RLCA.[17]

The relation between α and W_F (for several combinations of F_{ij} and D) is shown in Fig. 6, for three different values of the volume fraction. The values obtained for α do not systematically depend on φ and are in the same range as generally found. The parameters W_F and α are expected to be related, because the (early stage) growth of the clusters as a function of time, should depend on an effective stickiness of the particles. However, from the figure this is not clear.

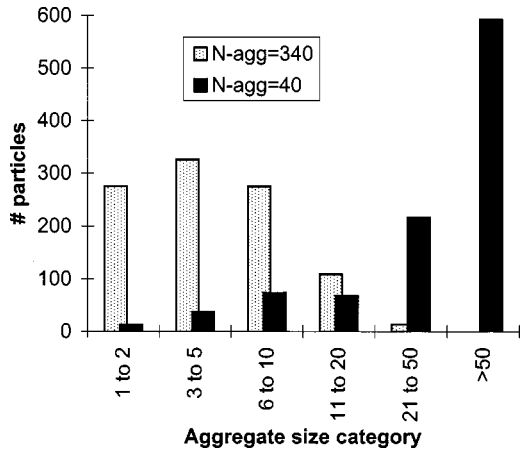

FIG. 2. Size distribution of the average total number of particles in aggregates at two stages during aggregation (at $N_{\mathrm{agg}}=340$ and 40).

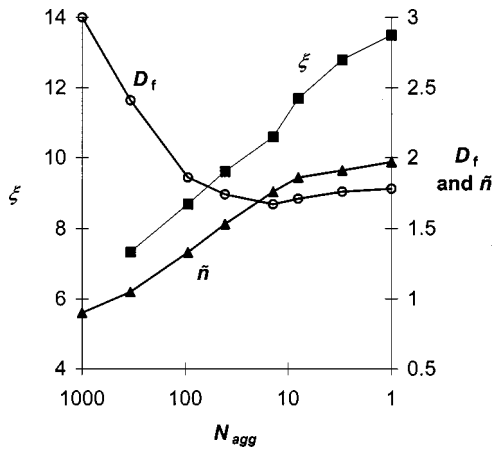

FIG. 4. Evolution of D_f, $\tilde{n}$ and ξ at $W_F=1$ and $\varphi=0.034$.

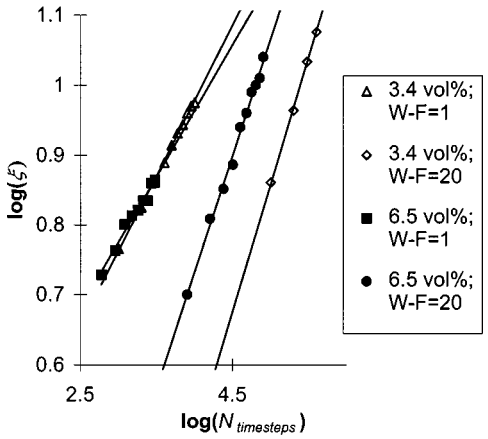

FIG. 5. Log(ξ) as a function of log($N_{\Delta t}$) at $\varphi=0.034$ ($W_F=1$ and 20) and $\varphi=0.065$ ($W_F=1$ and 20). The slope is equal to α.

Maybe, there is a leveling off of α at high values of W_F. The limit of $W_F \rightarrow 1$ corresponds to diffusion-limited behavior, so we can calculate a value of D_f according to $\alpha = 1/D_f$.[20] This leads to irrealistically large values for D_f, indicating that our situation is more complicated. Interestingly, we see from Fig. 6 that α is independent of W_F, at high (9.8 vol%) values of φ. The reason for this may have to do with limited formation of depletion zones at high φ, which we will discuss later.

In Figs. 7(a) and 7(b) we show projected images of the resulting structure of simulations performed at respectively $W_F=1$ and $W_F=20$. In both cases $N_{\text{agg}}=10$. Usually more than 90% of all particles are part of the largest aggregate at this stage of the aggregation process, so we speak of a gel. The images are projections along the z-axis. Shading is used as depth cueing. For more clear visualization, the particles are depicted at half their original size and a link is shown where a bond is present. The most clear difference between the images is that the pores in the gel seem larger at $W_F=20$, which is confirmed by a higher value of ξ. The two systems also have distinctly different D_f, but this is less clear from the image, probably because the fractal regime is relatively small.

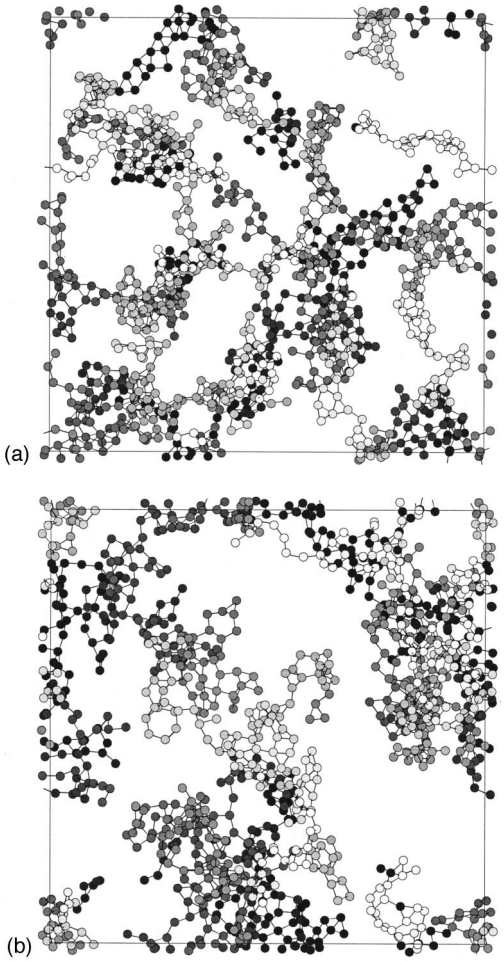

FIG. 7. Projected images of a simulated gels: (a) $W_F=1$; $D_f=1.7$; $\xi=11.5$ and (b) $W_F=20$; $D_f=2.1$, $\xi=22.3$.

In Fig. 8, the value of D_f at $N_{\text{agg}}=10$ is plotted against W_F for three different volume fractions. Each data point corresponds to one simulation with a certain value for D and F_{ij}. As we saw before,[8] D_f is related to W_F. At high W_F, D_f is systematically larger. At $W_F>5$ we see a leveling off of the curve. Important to note is that in the interaction range

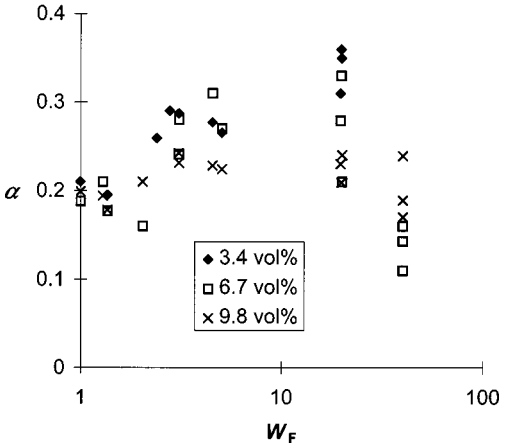

FIG. 6. The cluster growth exponent α as a function of W_F, at different volume fractions. Each data point corresponds to one simulation. Several combinations of F_{ij} and D were tested.

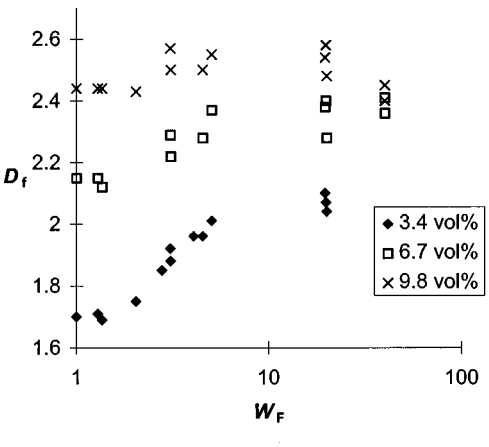

FIG. 8. The fractal dimensionality D_f at $N_{\text{agg}}=10$ as a function of W_F, at different volume fractions. Each data point corresponds to one simulation. Several combinations of F_{ij} and D were tested.

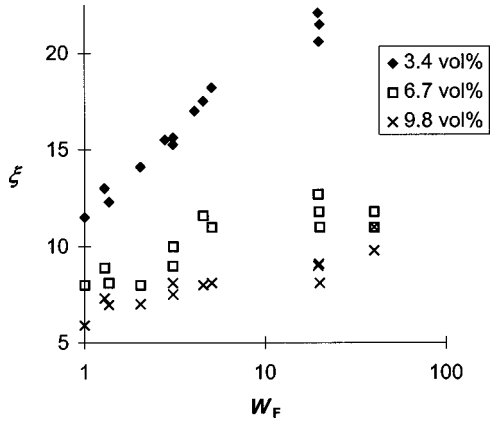

FIG. 9. The cluster radius at gelation, R_{gel}, as a function of W_F, at different volume fractions. Each data point corresponds to one simulation. Several combinations of F_{ij} and D were tested.

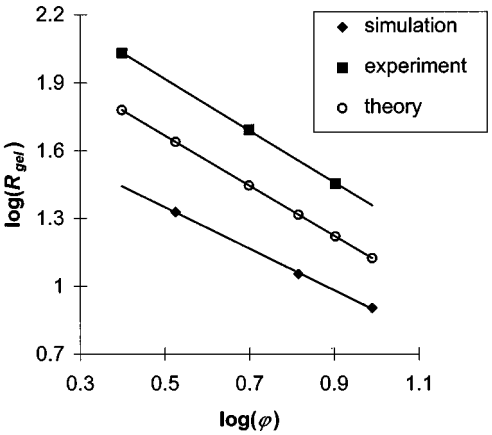

FIG. 10. Simulated R_{gel} as a function of φ. Also shown are lines according to Eq. (12) and experiments (Ref. 9).

studied, no systematic relation was found between the shape of the repulsive barrier and D_f. The fractal dimensionality D_f was not systematically higher or lower than the average behavior shown in Fig. 8, e.g., short-range repulsion.

In Fig. 9, the value of ξ at $N_{agg}=10$ ($\propto R_{gel}$) is plotted against W_F for three volume fractions. The correlation length ξ, and consequently R_{gel}, is larger at low φ, because gelation is reached at a later stage and the clusters are allowed to grow before they touch. In Fig. 9, we see a similar leveling off behavior as in Fig. 8. Not shown in the figure is that ξ is slightly higher for short-range repulsive barriers; i.e., most of the data points that are higher than the averages presented in Fig. 9, correspond to simulations incorporating a relative small value for the interaction range D.

The leveling-off behavior of Figs. 8 and 9 and the decreased dependency of D_f and ξ on W_F at high values of W_F, may be due to (a) larger fractal regimes at high W_F, and therefore more justified or accurate determination of these fractal parameters, or (b) the limited formation of ''depletion zones'' around the clusters compared to purely attractive systems. Maybe at high φ, both the fractal regime is larger and depletion zones can hardly develop.

We do not mean depletion zones due to an (entropic) volume exclusion effect, but due to a (kinetic) diffusion gradient effect. We expect that above a certain level of aggregation delay, there would be no depletion zones anymore. Similarly, fractal theory is mean field and may therefore only work properly if no strong density gradients are present at the surface of the clusters due to a reaction taking away particles (e.g., by aggregation) which is facter than the supply by diffusion. However, we have not checked explicitly for the existence of this type of depletion zones around clusters. Note that $n(r)$, which gives the average density distribution around fractal clusters, is always below the average bulk volume fraction φ near ξ, without showing clear depletion zones.

The decreased dependency of the fractal parameters on W_F at high W_F means that if we want to simulate, for instance, casein gels that are formed at a much slower rate than according to fast Smoluchowski kinetics, we probably do not have to incorporate the correct (very high) value for W_F to obtain reliable results, at least for the structural parameters discussed above.

At high W_F, the clusters formed and the pores in the gel are larger, but $\tilde{n}$ only increases slightly (implying that D_f is larger). Consequently, we find that the fractal scaling region is larger. In fact, $\tilde{n}$ decreases by about 10% for W_F ($1\rightarrow 20$), and is especially low at high D. The latter observation is in accordance with results of Meakin.[28] The decrease with increasing φ (e.g., $0.034\rightarrow 0.098$) is larger, namely by about 25% (data not shown). With increasing W_F, the structures are more tenuous at small length scales, and relatively homogeneous at intermediate (fractal) and large length scales.

We now define R_{gel} as the plateau value (i.e., at high W_F) of ξ at $N_{agg}=10$. In Fig. 10, we plotted this R_{gel} as a function of φ. Also plotted are the values of ξ from CSLM experiments on acid casein gels,[9] and a prediction using the fractal theory on R_{gel} according to Eq. (12), incorporating $a_{eff}=1$. We clearly see that the simulation and experimental results both have a scaling behavior predicted by incorporating $D_f=2.1$, which is a realistic value. In addition, the figure shows that ξ at $N_{agg}=10$ is smaller than may be expected, but roughly proportional to ξ determined in a fully developed gel. In addition, a larger value for a_{eff} which is more realistic for casein systems,[29,30] leads to a much better agreement between theoretical and experimental data.

In the simulations, rearrangements can only take place to a limited extent. This may account for differences in results between the simulations and experiments on practical systems. In our simulations (and other simulation studies[22,31]), rearrangements such as rolling or bending are accompanied by an increase in short-range compactness. Rheological and confocal experiments on rennet casein gels[30] show that extensive rearrangements induce syneresis and make the structures nonfractal, and this cannot happen in the simulations. These aging effects occur especially at low pH and high T (i.e., high particle affinity) and to simulate it, we probably have to incorporate particle fusion and breakage of strands.[30,32,33]

CONCLUSIONS

The cluster growth rate and the fractal properties of the gel matrix can be related to the particle interactions by approximating the simulation activation energies by a Fuchs stability ratio W_F.

Although the Fuchs approach would only apply to the very early stages of gelation, W_F was shown to be a useful parameter to obtain gel matrix parameters like the fractal dimensionality D_f and the correlation length ξ. The fractal parameters D_f and ξ systematically increase with W_F.

Interestingly, for high values for W_F, the value of D_f was more generic (i.e., less dependent of W_F or φ), possibly due to the limited formation of (kinetic) depletion or density gradient zones, compared to purely attractive systems. This is confirmed by the observation that also ξ and the cluster growth time scaling exponent α are less dependent of W_F at higher φ.

The distribution of the particles over the aggregates for the range of volume fractions and interactions studied was found to depend only on the number of aggregates, N_{agg}. We therefore conclude that the parameter N_{agg} is a good measure of the stage of aggregation, if we compare results of simulations at the same number of particles.

The results obtained cannot fully explain the behavior of rennet-induced casein gels and similar systems, probably because in this case other rearrangements than allowed in this study, like particle fusion and breaking of strands, are important in determining the final (fractal) structure.

ACKNOWLEDGMENTS

The authors wish to thank the European Union for financial support (FAIR-CT96-1216), and Pieter Walstra (Wageningen, The Netherlands) for helpful and stimulating discussions.

[1] E. Dickinson, J. Chem. Soc., Faraday Trans. **90**, 173 (1994).
[2] B. H. Bijsterbosch, M. T. A. Bos, E. Dickinson, J. H. J. van Opheusden, and P. Walstra, Faraday Discuss. **101**, 51 (1995).
[3] M. T. A. Bos and J. H. J. van Opheusden, Phys. Rev. E **53**, 5044 (1996).
[4] J. F. M. Lodge and D. M. Heyes, J. Chem. Soc., Faraday Trans. **93**, 437 (1997).
[5] M. Whittle and E. Dickinson, Mol. Phys. **5**, 739 (1997).
[6] C. M. Wijmans and E. Dickinson, J. Chem. Soc., Faraday Trans. **94**, 129 (1998).
[7] J. F. M. Lodge and D. M. Heyes, J. Rheol. **43**, 219 (1999).
[8] M. Mellema, J. H. J. van Opheusden, and T. van Vliet, in *Food Emulsions and Foams: Interfaces, Interactions and Stability*, edited by E. Dickinson and J. M. Rodriguez Patino (Royal Society of Chemistry, Cambridge, 1999).
[9] M. T. A. Bos, Ph.D. Thesis, Wageningen Agricultural University, 1997.
[10] C. Holt and D. C. Horne, Neth. Milk Dairy J. **50**, 85 (1996).
[11] M. D. Haw, M. Sievwright, W. C. K. Poon, and P. N. Pusey, Adv. Colloid Interface Sci. **62**, 1 (1995).
[12] L. G. B. Bremer, Ph.D. Thesis, Wageningen Agricultural University, 1992.
[13] T. A. J. Payens, Biophys. Chem. **6**, 263 (1977).
[14] A. C. M. van Hooydonk and P. Walstra, Neth. Milk Dairy J **41**, 19 (1987).
[15] M. Mellema, F. A. M. Leermakers, and C. G. de Kruif, Langmuir (accepted for publication).
[16] L. G. B. Bremer, B. H. Bijsterbosch, P. Walstra, and T. van Vliet, Adv. Colloid Interface Sci. **46**, 117 (1993).
[17] H. Y. Lin, H. M. Lindsay, D. A. Weitz, R. C. Ball, R. Klein, and P. Meakin, Phys. Rev. A **41**, 2005 (1990).
[18] N. Fuchs, Z. Phys. **89**, 736 (1934).
[19] M. P. Allen and D. J. Tildesley, *Computer Simulation of Liquids* (Oxford Science Publications, 1987).
[20] P. Meakin, Adv. Colloid Interface Sci. **28**, 249 (1988).
[21] P. Meakin, Heterog. Chem. Rev. **1**, 99 (1994).
[22] P. Meakin and R. Jullien, J. Phys. (France) **46**, 1543 (1985).
[23] M. Smoluchowski, Z. Phys. Chem. (Leipzig) **92**, 129 (1917).
[24] T. F. Tadros, Adv. Colloid Interface Sci. **68**, 97 (1996).
[25] B. B. Mandelbrot, *The Fractal Geometry of Nature* (Freeman, New York, 1982).
[26] E. Dickinson, in *Food Colloids: Proteins, Lipids and Polysaccharides*, edited by E. Dickinson and B. Bergenståhl (Royal Society of Chemistry, Cambridge, 1997).
[27] M. Carpineti and M. Giglio, Adv. Colloid Interface Sci. **46**, 73 (1993).
[28] P. Meakin, J. Colloid Interface Sci. **134**, 235 (1990).
[29] T. van Vliet, J. A. Lucey, K. Grolle, and P. Walstra, in *Food Colloids; Proteins, Lipids and Polysaccharides*, edited by E. Dickinson and B. Bergenståhl (Royal Society of Chemistry, Cambridge, 1997).
[30] M. Mellema, J. H. J. van Opheusden, and T. van Vliet (unpublished).
[31] P. W. Zhu and D. H. Napper, Phys. Rev. E **50**, 2 (1994); **50**, 1360 (1994).
[32] S. P. F. M. Roefs, T. van Vliet, H. J. C. M. van den Bijgaart, A. E. A. de Groot-Mostert, and P. Walstra, Neth. Milk Dairy J **44**, 159 (1990).
[33] T. van Vliet, H. J. M. van Dijk, P. Zoon, and P. Walstra, Colloid Polym. Sci. **269**, 620 (1991).